

Automotive Body Design

Jeong-Ick Lee*, Byoun-Gon Kim**, Tae-Jin Chung**

(논문접수일 2007. 12. 3, 심사완료일 2008. 5. 2)

차량 차체 설계

이정익*, 김병곤**, 정태진**

Abstract

In an automotive body structure, a design configuration that fulfills structural requirements such as deflection, stiffness and strength is necessary for structural design and is composed of various components. The integrated design is used to obtain a minimum weight structure with optimal or feasible performance based on conflicting constraints and boundaries. The mechanical design must begin with the definition of one or more concepts for structure and specification requirements in a given application environment. Structural optimization is then introduced as an integral part of the product design and used to yield a superior design to the conventional linear one. Although finite element analysis has been firmly established and extensively used in the past, geometric and material nonlinear analyses have also received considerable attention over the past decades. Also, nonlinear analysis may be useful in the area of structural designs where instability phenomena can include critical design criteria such as plastic strain and residual deformation. This proposed approach can be used for complicated structural analysis for an integrated design process with the nonlinear feasible local flexibilities between system and subsystems.

Key Words : sequential configuration design(연속 형상 설계), substructures(하부 구조), plastic strain(소성 변형), idle shake, (여 진동), wheel unbalance shake(바퀴 불균형 진동), road shake(주행 진동)

Notation

		$\{x\}$	State parameter vector
		$\{F\}$	Force vector
$[K]$	Stiffness matrix	$\{\phi\}$	Normal mode vector
$[M]$	Mass matrix	$[H]$	Frequency response function

* 인하공업전문대학 기계시스템학부 기계설계과 (jilee@inhac.ac.kr)

주소: 402-752 인천광역시 남구 용현동 253번지

** 군산대학교, 기계공학과

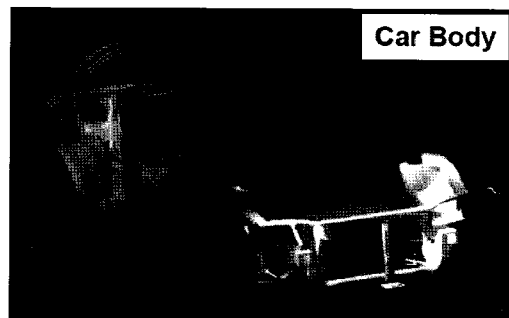
- b Design parameter
- Π Driving point residue
- Ψ Objective function
- ζ Modal damping ratio

1. Introduction

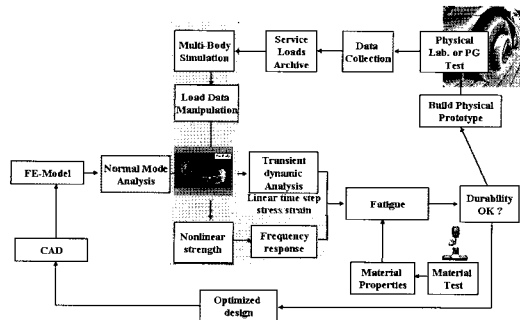
The automotive body must fulfill mechanical performance requirements such as deflection, stiffness and strength, in an extensive amount of structural design considerations and components. It becomes important that the integrated design is used to obtain a minimum weight structure with maximum or feasible performance based on the conflicting constraints and boundaries. Thus, the mechanical design must begin with the definition of one or more concepts for system or subsystems and a quantitative specification citing requirements, in a given application environment. The overall problem is broken into a series of related but independently definable parts based on the subsystem decomposition, without the vague concepts of system or subsystem definition. Two of the most important inputs to the design process are the performance specification and the definition of imposed constraints. The former is the prospective user's definition of how the performance specification will be acceptable, whereas the latter defines the physical limitations such as size, weight, configuration and environment that affect the mechanical interfaces. Given sets of specifications and constraints as well as configuration subsystems, the idealized design process proceeds into the preliminary design phase. The main purpose of optimization design is to reduce risk associated with the introduction of new or improved products into the production. Generally, structural properties have either local design parameters or global design parameters in each design stage. In local design parameters, the detailed dimensions of subsystems are used to generate the intermediate structural properties^(1,2). In global design parameters, structural properties are themselves used as the design parameters⁽³⁻⁶⁾. However, for the efficiencies of computations and making- decisions, both types of design parameters

must have the feasible limitations at the number and region. The local and global design parameters are interrelated in an integrated optimization procedure for incorporating dynamic and structural performances^(6-8,10-15). The function of the component to be designed is examined in more detail and the technical specifications begin to take form. Therefore, the parametric trade-off analysis based on the structural dimensions and properties are performed in order to develop the interrelations between parameters.

The paper presents the design process for the integrated configuration of subsystem and system presented previously⁽¹³⁻¹⁵⁾. In order to obtain the feasible responses of subsystems, a subsystem design model considering the flexibility of the main structure is basically built through static or modal analysis and using such design parameters as thickness and geometric dimensions, the dynamic response of system is investigated. For the feasibility design of the subsystem, the local flexibility effects are taken into account. Figure 1 shows the running simulation



(a) Full automotive model using modal flexible BIW



(b) Integration design scheme

Fig. 1 Virtual running simulation of full automotive model

and integration design scheme for the nonlinear strength, frequency response and durability using the modal flexible body. These maximum durability load characteristics are given from the virtual running simulation of full automotive model with the modal flexible body as shown in figure 1-(a) used at the commercial software. In this paper, the nonlinear specifications of front control arm and the vibration specifications of automotive body are used in the design development process. The overall integrated design process used in this paper is shown in figure 2. For the screening of design parameters in the subsystems, DOE (design of experiments) is used in the nonlinear structural performances of front control arm and vibrations of automotive body. Each design parameter set is integrated in the system level.

2. Theoretical Considerations of Local Flexibilities

In the substructuring design, the following contents are explained for the local flexibilities.

2.1 Static analysis

The subsystem is based on decomposition of the original structure into several subsystems and load transfers as shown in Figure 3. Let us assume the system of linear algebraic equations.

$$[K]\{x\} = \{F\} \quad (1)$$

where the matrix of system $K \in \mathfrak{R}^{n \times n}$ and vectors $x \in \mathfrak{R}^n$, $F \in \mathfrak{R}^n$

It is possible to split original system into subsystem blocks.

$$\begin{bmatrix} K^{AA} & K^{AB} \\ K^{BA} & K^{BB} \end{bmatrix} \begin{Bmatrix} x^A \\ x^B \end{Bmatrix} = \begin{Bmatrix} F^A \\ F^B \end{Bmatrix} \quad (2)$$

If the block K^{AA} is regular, the vector x^A can be expressed from the first matrix equation and has a form,

$$\{x^A\} = [K^{AA}]^{-1} \{F^A - [K^{AB}]\{x^B\}\} \quad (3)$$

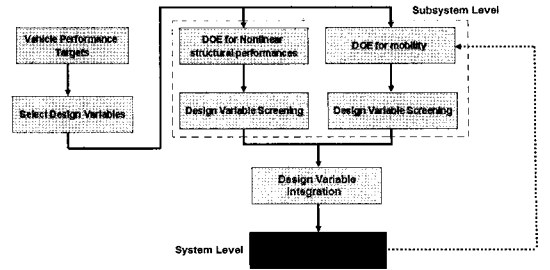


Fig. 2 Process for integrated configuration design of automotive chassis parts

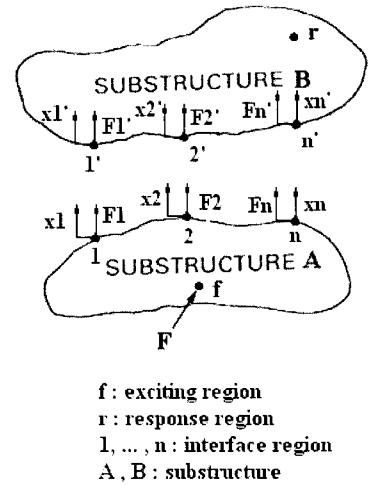


Fig. 3 Load transfer in structure system

The second equation of the original system has a modified form after substitution into eq. (3).

$$\begin{aligned} [K^{BB} - K^{BA}[K^{AA}]^{-1}K^{AB}]\{x^B\} &= \{F^B - [K^{BA}[K^{AA}]^{-1}]\{F^A\}\} \\ [K^{BB} - K^{BA}[K^{AA}]^{-1}K^{AB}]\{x^B\} &= \{F^B - [K^{BA}[K^{AA}]^{-1}]\{F^A\}\} \end{aligned} \quad (4)$$

The matrix $[K^{BB} - K^{BA}[K^{AA}]^{-1}K^{AB}]$ is called static condensation and the boundary interfaces have influences on the substructure responses. Figure 4 shows the interfaces of subsystems with the stiffness and damping among substructures.

The physical degrees of freedom of the analysis set can

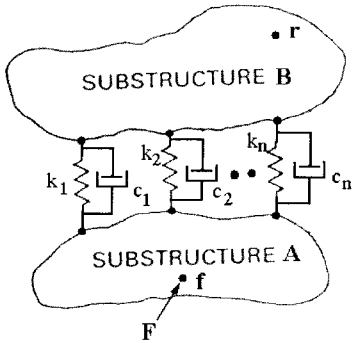


Fig. 4 Interface of substructures

be reduced to a smaller set consisting of physical interface degrees of freedom as follows.

$$[K^*]\{x^B\} = \{F^*\} \quad (5)$$

where

$$[K^*] = [K^{BB} - K^{BA}[K^{AA}]^{-1}K^{AB}]$$

$$\{F^*\} = \{F^B - [K^{BA}[K^{AA}]^{-1}\{F^A\}]\}$$

The gradient of response function with respect to the design parameter b can be given by.

$$[K^*] \frac{\partial \{x^B\}}{\partial b} = \frac{\partial \{F^*\}}{\partial b} - \frac{\partial [K^*]}{\partial b} \{x^B\} = \{\tilde{F}\} \quad (6)$$

2.2 Normal mode analysis

In the substructure system, the mass and stiffness matrices may be reordered, placing all degrees of freedom that are joined with substructures by using a vector matrix through the transformation. The mass and stiffness matrices may be partitioned to form,

$$[M] = \begin{bmatrix} M^{AA} & M^{AB} \\ M^{BA} & M^{BB} \end{bmatrix}, \quad [K] = \begin{bmatrix} K^{AA} & K^{AB} \\ K^{BA} & K^{BB} \end{bmatrix}$$

For a redundant connection between substructures, there exists a set of constraint modes, ϕ_c , which are the deflections of the internal degrees of freedoms due to a unit displacement of each of the interface degrees of

freedom. They can be written as,

$$[\phi_c] = -[K^{BB}]^{-1}[K^{BA}] \quad (7)$$

The normal vector of elastic modes for this system, as if the interface degrees of freedom were constrained, ϕ_n , can be also be obtained, by solving the eigenvectors of the system.

$$[K^{BB} - \lambda_n M^{BB}]\{\phi_n\} = \{0\} \quad (8)$$

A transformation matrix can then be formed using these two mode shapes, namely;

$$[T] = \begin{bmatrix} I & 0 \\ \phi_c & \phi_n \end{bmatrix} \quad (9)$$

Using this transformation, the physical degrees of freedom of the analysis set can be reduced to a smaller set consisting of physical interface degrees of freedom and a set of generalized coordinates by the triple products.

$$[M^*] = [T]^T [M] [T], \quad [K^*] = [T]^T [K] [T] \quad (10)$$

This reduction procedure is performed for substructures and the matrices are to be joined for the coupled analysis. To perform the coupled modal analysis, the reduced mass and stiffness matrices are merged with the interfaces among substructures. The gradient of response function with respect to the design parameter b can be given by.

$$\frac{\partial \lambda_n}{\partial b} = \frac{\{\phi_n\}^T \left(\frac{\partial [K^*]}{\partial b} - \lambda_n \frac{\partial [M^*]}{\partial b} \right) \{\phi_n\}}{\{\phi_n\}^T [M^*] \{\phi_n\}}$$

$$= \{\phi_n\}^T \frac{\partial [K^*]}{\partial b} \{\phi_n\} - \lambda_n \{\phi_n\}^T \frac{\partial [M^*]}{\partial b} \{\phi_n\} \quad (11)$$

where $\{\phi_n\}^T [M^*] \{\phi_n\} = 1$

2.3 Frequency response analysis

Figure 4 shows the system with two substructure and connection elements. When the external force (F) is acted at the point f of substructure A , the response at the point r of substructure B can be defined by the transfer

functions of substructures and connection characteristics. Under the load condition of F at the point f , the responses of connection points on the substructure A can be given by,

$$\{x_i^A\} = [H_{ij}^A]\{F\} + [H_{ij}^A]\{R_j\} \quad \begin{matrix} i=1, \dots, n \\ j=1, \dots, n \end{matrix} \quad (12)$$

where H_{ij}^A is the frequency response function, the index A represents the substructure, the index i represents the response point, the index j represents the loading point and R_j is the reaction force at the connection point j .

The responses at the connection points j and r on the substructure B can be given by,

$$\{x_j^B\} = -[H_{ij}^B]\{R_j\}, \quad \begin{matrix} i=1, \dots, n \\ j=1, \dots, n \end{matrix} \quad (13)$$

$$\{x_r^B\} = -[H_{rj}^B]\{R_j\}, \quad r=1, \dots, n \quad (14)$$

If two substructures are elastically connected, the relationship between two substructures is as follows.

$$[K_{ij}^I]\{R_j\} = \begin{Bmatrix} x_1^B \\ \vdots \\ x_n^B \end{Bmatrix} - \begin{Bmatrix} x_1^A \\ \vdots \\ x_n^A \end{Bmatrix}, \quad \begin{matrix} i=1, \dots, n \\ j=1, \dots, n \end{matrix} \quad (15)$$

$$\text{where } [K_{ij}^I] = \begin{cases} \frac{1}{(k_i + j\omega c_i)}, & \text{if } i=j \\ 0, & \text{if } i \neq j \end{cases}$$

Using eq. (12), (13) and (14), the reaction force at each connection point can be given by,

$$\{R_j\} = -[K_{ij}^{-1}][H_{ij}^A]\{F\}, \quad i=1, \dots, n \quad (16)$$

$$\text{Where } [K_{ij}] = [K_{ij}^I] + [H_{ij}^A] + [H_{ij}^B] \quad (17)$$

From eq. (14), the gradient of response function with respect to the design parameter b can be given by.

$$\frac{d\{x_r^B\}}{db} = -\frac{\partial[H_{rj}^B]}{\partial b} \cdot \{R_j\} - [H_{rj}^B] \cdot \frac{\partial\{R_j\}}{\partial b} \quad (18)$$

The gradient of reaction force with respect to the design parameter b can be written by eq. (16).

$$\frac{\partial\{R_j\}}{\partial b} = -[K_{ij}]^{-1} \left\{ \frac{\partial[K_{ij}]}{\partial b} \cdot [R_j] + \frac{\partial[H_{ij}^A]}{\partial b} \{F\} + [H_{ij}^A] \frac{\partial\{F\}}{\partial b} \right\} \quad (19)$$

Because the loading condition is constant, $\frac{\partial F}{\partial b}$ is zero. eq. (18) can be written by.

$$\frac{d\{x_r^B\}}{db} = -\frac{\partial[H_{rj}^B]}{\partial b} \cdot \{R_j\} + [H_{rj}^B] \cdot [K_{ij}]^{-1} \left\{ \frac{\partial[K_{ij}]}{\partial b} \cdot \{R_j\} + \frac{\partial[H_{ij}^A]}{\partial b} \{F\} \right\} \quad (20)$$

Because the right-hand side terms of eq. (20) can be calculated, the gradient of response function is found. Through the sensitivity analysis, the feasibility design of substructure can be made.

3. Design Optimization Process

The design process for mechanical systems can be viewed as an optimization process to find parts that fulfill certain quality requirements towards their functionality, appearance and economy. It can be described as an iterative search process⁽¹⁶⁻¹⁹⁾ that uses the following steps:

1. Define an initial design $b^{(i=0)}$
2. Analyze the properties of the components
3. Compare the results of the analysis with the requirements such as allowable static and dynamic performances

Of the requirements are not met, change the design such that $b^{(i+1)} = b^{(i)} + \delta b$

The general formulation of an optimization problem appears as

$$\text{Minimize } \psi_0(b)$$

$$\text{subject to } \psi_i(b) \leq 0, \quad b^L \leq b \leq b^U$$

Objective and constraints $\psi_i(b)$, $i=0, \dots, n$ can be approximated for each design $b^{(i)}$ using the series expansion,

$$\psi_i = \psi_i(b^{(i)}) + \sum_{j=1}^m \frac{d\psi_i}{db_j} \delta b_j \quad (21)$$

The gradient $\frac{d\psi_i}{db_j}$ can be obtained directly from the results of finite element analysis. If the gradient is known, the search direction δb can be obtained from the solution of an approximate optimization problem

4. Simulation

4.1 Nonlinear material specifications

In the nonlinear material specifications, we can consider the displacement motion of a structure under body force F^B and surface traction F^S on the surface S . The Lagrangian approach is used to formulate the nonlinear problem because its formulation is usually reasonable and effective. In the Lagrangian approach, the equilibrium of the body can be expressed by the principle of virtual displacements.

$$\begin{aligned} W &= \int_V \sigma_{ij} \Delta \varepsilon_{ij} dV \\ &= \int_V F_i^B \Delta u_i^B dV + \int_S F_i^S \Delta u_i^S dS \end{aligned} \quad (22)$$

where W is the mean compliance, σ_{ij} is the stress tensor, $\Delta \varepsilon_{ij}$ is the incremental strain tensor corresponding to virtual displacement, Δu_i^B and Δu_i^S are the virtual displacements.

The strain tensor is defined with respect to the initial coordinates of the body

$$\Delta \varepsilon_{ij} = \frac{1}{2} \left(\frac{\partial \Delta u_i}{\partial x_j} + \frac{\partial \Delta u_j}{\partial x_i} + \frac{\partial \Delta u_k}{\partial x_i} \frac{\partial \Delta u_k}{\partial x_j} \right) \quad (23)$$

$$\{\Delta \varepsilon\} = [B] \{\Delta u\} = ([B_L] + [B_{NL}]) \{\Delta u\} \quad (24)$$

where $[B]_L$ and $[B]_{NL}$ represent spatial derivatives of linear small and nonlinear large displacement.

If strains are very small, we can write the general elastic constitutive relation.

$$\sigma_{ij} = C_{ijkl} \varepsilon_{kl} \quad (25)$$

where C_{ijkl} is the constant elasticity tensor.

In order to calculate the structural responses using geometrical and material nonlinear analysis, nonlinear terms in eq. (22) and (23) are considered. However, they cannot be solved directly due to their high degree of nonlinearities. Therefore, linearization can be used as an approximation solution. For optimizing the design of a structure under a given load, the mean compliance is defined as the objective function. For deriving the strain energy in terms of nonlinearities, we need to reformulate W in terms of stress and strain. From eq. (22) and (23), we can have

$$W = \int_V \sigma_{ij} \left(\Delta \varepsilon_{ij}^L + \frac{1}{2} \frac{\partial \Delta u_k}{\partial x_i} \frac{\partial \Delta u_k}{\partial x_j} \right) dV \quad (26)$$

where $\Delta \varepsilon_{ij}^L$ is the elastic strain.

In the sensitivity analysis of mean compliance, $\frac{dW}{dp}$ can be expressed as

$$\begin{aligned} \frac{dW}{dp} &= \frac{d}{dp} \int_V \sigma_{ij} \left(\Delta \varepsilon_{ij}^L + \frac{1}{2} \frac{\partial \Delta u_k}{\partial x_i} \frac{\partial \Delta u_k}{\partial x_j} \right) dV \\ &= \int_V F_i^B \frac{\partial \Delta u_i^B}{\partial p} dV + \int_S F_i^S \frac{\partial \Delta u_i^S}{\partial p} dS \end{aligned} \quad (27)$$

where p is the design parameter.

Substituting eq. (24) into the linearized equilibrium equation, we can state the incremental description as

$$[K_T] \{\Delta u\} = \{\Delta F\} \quad (28)$$

where $[K_T]$ is known as the tangent stiffness matrix

which is calculated by adding the elastic material matrix and the second Piola-Kirchhoff stress matrix to the strain-displacement transformation matrices:

$$\begin{aligned} [K_T] &= [K_L] + [K_{NL}] \\ &= \int_V [B_L + B_{NL}]^T [D] [B_L + B_{NL}] dV \\ &= \int_V [B_L]^T [D] [B_L] dV + \left\{ \int_V [B_L]^T [D] [B_{NL}] dV \right. \end{aligned}$$

$$+ \int_V [B_{NL}]^T [D][B_L] dV + \int_V [B_{NL}]^T [D][B_{NL}] dV \} \quad (29)$$

$[K_L]$ denotes the small displacement stiffness and $[K_{NL}]$ denotes the large displacement and nonlinear material behaviors.

The residual between the external and internal forces is represented by $\{\Delta F\}$ as follows:

$$\{\Delta F\} = \int_V f^B \Delta u^B dV + \int_S f^S \Delta u^S dV - \int_V \bar{\sigma} [B_L + B_{NL}] dV \quad (30)$$

where $\bar{\sigma}$ is the stress tensor in the iterative nonlinear process resulting in the internal forces

Consider the nonlinear force-deformation relationship in shown Fig. 1. We imagine that the tangent stiffness can be composed of the linear term $[K_L]$ and the nonlinear term $[K_{NL}]$ that affect the deformations with geometric and material nonlinearities. In the force-deformation relationship, $[K_L]$ and $[K_{NL}]$ are known as the functions of $\{\Delta u\}$ relative to the structural rigidities due to the geometric dimensions and therefore, $\{\Delta F\}$ can also be calculated in terms of geometric dimensions.

The nonlinear material specifications of most automotive components must be evaluated for their durability and strength. The loading cases will generally be provided by the buyer. The scaled loading condition is commonly used as a guideline for durability assessment⁽¹³⁾. In this model, three times gross vehicle weight (GVW) in the lateral direction and 2.5 times GVW in the backward direction are used to estimate maximum durability and the structural specification of the control-arm must satisfy the nonlinear target specifications. Figure 5 shows the finite element model of a front cross-member assembly (ASM) with mounting bushes. The maximum loads used in the loading and unloading are acted in the wheel center and their effects are transferred to the control-arm. For comparison with a designed control-arm, 25 measuring points are chosen as shown in figure 6(a). For acceptable durability, the control-arm must have the allowable plastic strain. In order to design the control-arm with the

allowable plastic strain, the design parameters are chosen to be the upper and lower panel thickness (t) and inner section dimensions-height (h) and width (w)-with curved bead as shown in figure 6-(b). The shape directions in the inner section of the control-arm near the vertical

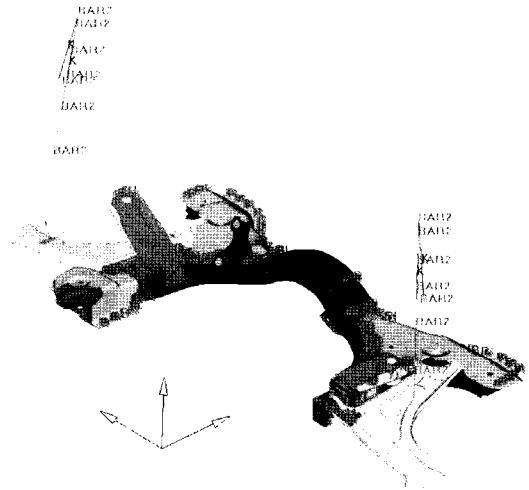
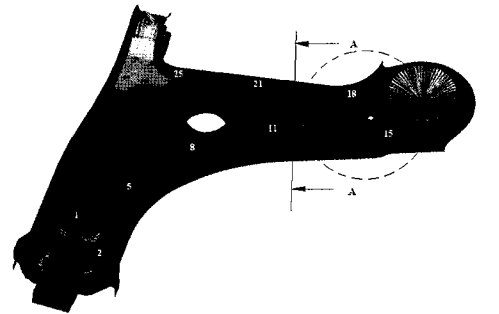
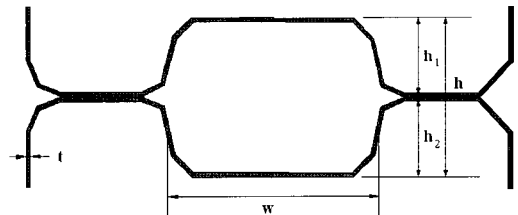


Fig. 5 Front cross-member ASM



(a) Measuring points and designed zone



(b) Design parameters of section A-A

Fig. 6 Design parameter and measuring points of control-arm

mounting bushing can be defined by setting the basis vector of grid point changes to the directions normal to the surfaces as follows:

$$\{\Delta G\} = [T] \{\Delta p\} \quad (31)$$

where $\{\Delta G\}$ is the set of grid point changes, $[T]$ is the set of shape basis vectors and $\{\Delta p\}$ is the set of scaled design parameter changes in the geometric dimensions of shape.

The objective of the function is to minimize the mean compliance with the weight of the control-arm. The constraints must be below 4% equivalent plastic strain (ε^p), and the material properties are shown in Table 1.

Minimize $W(p)$

subject to $\varepsilon^p \leq \varepsilon^p_{given}$

$$2.0 \leq t \leq 2.5,$$

$$40. \leq w \leq 45.,$$

$$20. \leq h \leq 24.$$

For the nonlinear optimization, the external optimizer and NX. Nastran are used. Boundary conditions are given on the actual running motions of automotive structure.

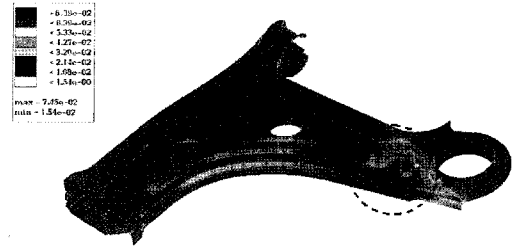
Figure 7 shows the contour of equivalent plastic strain calculations of the initial design and the discrete-optimum design. Table 2 shows the parameters and plastic strains between the initial and optimum design. Compared to the initial design, 48% of the plastic strain is removed and the weight reduction is 8% in the optimum design.

4.2 Vibration specifications

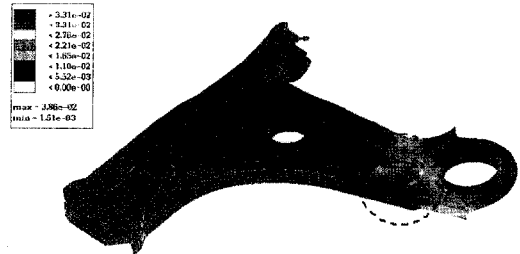
Frequency in the dynamic characteristics of the automotive body is one of the most important factors influencing the overall NVH (Noise, Vibration and Harshness) quality of a passenger vehicle^(14,15). In particular, the driver is sensitive to the vibrations of the steering wheel in the frequency range of engine idle shake, wheel shake, and road shake. By controlling these kinds of vibrations and understanding the current phenomena in more detail, a well-correlated finite-element model can

Table 1 Material properties

	E(GPa)	Poisson's ratio, ν	Density, ρ (ton/m ³)	σ_y (MPa)
value	204	0.3	7.85	385



(a) Equivalent plastic strain of initial design



(b) Equivalent plastic strain of discrete optimum design

Fig. 7 Plastic strain contour of control-arm

Table 2 Design parameters and plastic strains in the design process

Design	t(mm)	w(mm)	h(mm)	Max. plastic strain(%)
Initial	2.5	40	20	7.45
Optimum	2.28	43.8	23.8	3.28
Discreat	2.3	44	24	3.25

be found. Although deciding what the parameters are relatively simple, deciding how to apply them to a realistic model is a different problem in terms of feasibility and reliability. To obtain a reliable model, a total vehicle

model with main components shown in figure 8 was validated with test results as shown in Table 3. The suspension system, exhaust system and steering system are shown in Figure 8 as the chassis system attached to B.I.W.. The correlation between the test model and the finite element model was validated by Modal Assurance Criteria (MAC) in eq. (32). MAC values in the range of frequencies appear to be more than 80% and this model is available for a feasible vehicle design study.

$$MAC_{jk} = \frac{|\phi_{ij}^T \phi_{ak}|^2}{(\phi_{ak}^T \phi_{ak})(\phi_{ij}^T \phi_{ij})} \quad (32)$$

This simulation modeled the vibration characteristics with respect to engine idle shake, wheel shake, and road

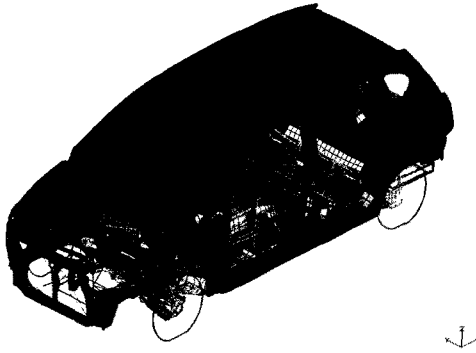


Fig. 8 Total vehicle model

Table 3 Modal assurance criteria of the updated vehicle model

Reference frequency range (TEST, Hz)	Verification frequency range (FEM, Hz)	MAC Value (%) ($j=k$)
24.47	24.38	0.95
25.76	26.22	0.93
29.77	30.03	0.85
32.75	32.98	0.86
37.65	38.42	0.88
39.47	40.02	0.83
42.45	43.18	0.84

shake. Engine excitation can be divided into two components: the unbalanced force due to the vertical force of the piston, and the torque fluctuation due to pressure within the cylinders and the rotational moment.

For the unbalanced force, we have:

$$F = 4(m_{piston} + m_{conrod}) \frac{R^2 \omega^2}{L^2} \cos 2\omega t \quad (33)$$

For torque fluctuation, we have:

$$M = -2(m_{piston} + m_{conrod}) \omega^2 R^2 \sin 2\omega t \quad (34)$$

where m_{piston} and m_{conrod} are the piston mass and connecting rod mass, R is the crank radius, L is the connecting rod length, ω is the angular velocity.

The excitations of wheel unbalance shake acted on the LH and RH front wheels with an unbalanced mass of 60 gram:

$$F = M r \omega^2 \quad (35)$$

where M is the unbalanced mass of the tire wheel, r is the radius of the wheel rim and ω is the angular velocity of the wheel.

Road shake is formulated by the excitation from the road running profile and the force amplitude is vertically applied at the hub used in the automotive maker.

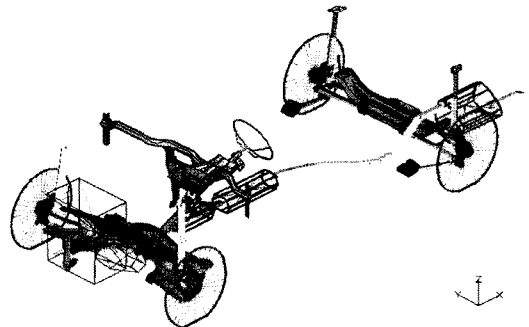


Fig. 9 Chassis system with suspension, exhaust and steering system

$$F = C |freq|^n \quad (36)$$

where C and n are 353.84 as the excitation load and 0.7120543 as the exponent of frequency from the relationship curves between road running frequencies and excitation load transferred to the hub, respectively on the ground of experiments specified in the automotive maker. They are correlated from the running test⁽¹⁵⁾.

To analyze the dynamic stiffness of the vehicle body, sinusoidal forces were applied at the engine excitation point and the wheel rims. The accelerations of the steering wheel and body C.G. (Center of Gravity) point were calculated in the frequency range of 0~800 RPM. The multi-criteria optimization of panel thickness, average bush stiffness, and floor panel bead were performed for increasing dynamic stiffness. The damping ratio was set at 3% for the frequency range of interest. The optimization problem was to find the panel thickness, floor panel bead dimensions, and average bush stiffness that minimizes initial acceleration under a given frequency range, which includes the excitation by idle shake (f_{idle}), wheel shake (f_{wheel}), and road shake (f_{road}). The available design parameters were 14 panel thicknesses, 13 beads, and 3 average bush stiffness.

$$\begin{aligned} \text{Minimize } F(X) &= w_1 f_{idle}(X) + w_2 f_{wheel}(X) + w_3 f_{road}(X) \\ \text{for } \sum_{i=1}^3 w_i &= 1 \end{aligned} \quad (37)$$

$$\begin{aligned} \text{subject to } 0.8 \cdot (t_i)_0 &\leq t_i \leq 1.2 \cdot (t_i)_0 \\ 0.9 \cdot (k_{bush 0})_j &\leq (k_{bush})_j \leq 1.5 \cdot (k_{bush 0})_j \end{aligned}$$

Beaded floor panels have been widely incorporated into automotive designs to improve dynamic stiffness. The floor panel is designed to minimize its local deformation in the desired frequency range. The bead pattern can be defined parametrically in terms of length, width, and height. The thickness of the floor panel was included in the sizing optimization. Figure 10 shows bead parameters built on a flat floor: w_0 and w_1 are the bead's base and top width, respectively, and H and L are the bead's height and length, respectively. The height and width of

the bead cannot be changed arbitrarily because of manufacturing limitations. After carefully considering the involved factors, a cross section must be chosen. The lengths of beads are pre-chosen in the topology optimization. The geometrical constraints of bead parameters are as follows:

$$\text{For each bead, } h^L \leq \text{change of height } (h) \leq h^u$$

$$w^L \leq \text{change of width } (w) \leq w^u$$

$$a^L_j \leq \text{configuration vector } (a_j) \leq a^u_j, j=1 \dots n$$

where h and w are the dimensions of the reinforced bead

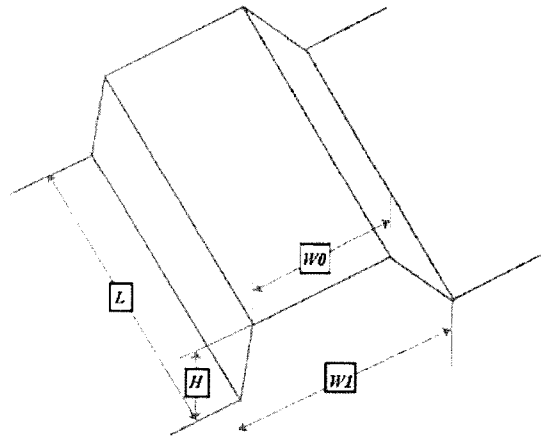


Fig. 10 Definitions of bead parameters

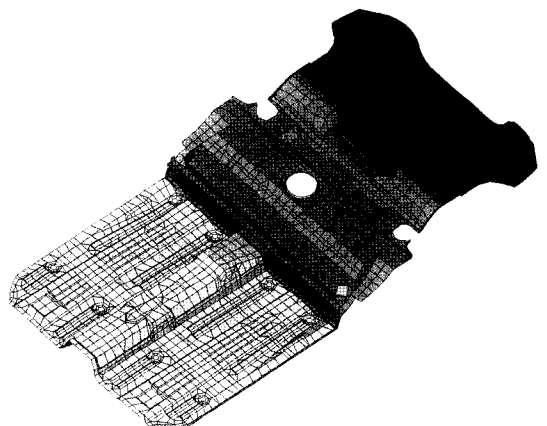


Fig. 11 Beaded floor panel

Table 4 Design parameters in initial and optimization design (Units; mm)

Design	Initial design	Optimized design
Dash cross member	1.50	1.00
Dashpanel	0.85	0.80
Front rail BRKT at Dash	1.40	1.30
Shock tower front UPR	2.35	1.75
Shock tower LWR	2.35	1.85
Fender support rail	0.80	0.80
Hinge pillar INR	0.80	0.85
Hinge pillar OTR	1.00	1.15
Front rail	1.20	1.30
Skirt	0.65	0.85
Steering column SPRT BRKT	1.60	1.85
Steering column BAR	2.00	2.00
Engine MTG Bush stiffness LH	171	165
Engine MTG Bush stiffness RH	125	130
Engine MTG Bush stiffness RR	140	150
Front floor panel	1.85	1.80
Rear floor panel	1.85	1.75

in the inner panel, and a_j is the move vector of the bead shape.

Figure 11 shows the beaded floor panel made through multi-criteria optimization. Table 4 shows the design parameters of the initial and optimized designs. Figure 12 shows the acceleration at the steering center and the body CG. The optimized design shows marked improvement in acceleration over the baseline model.

The design parameters shown in Table 4 are simulated on the mounting local flexibilities between system and subsystem through the sequential design process shown in Fig. 2.

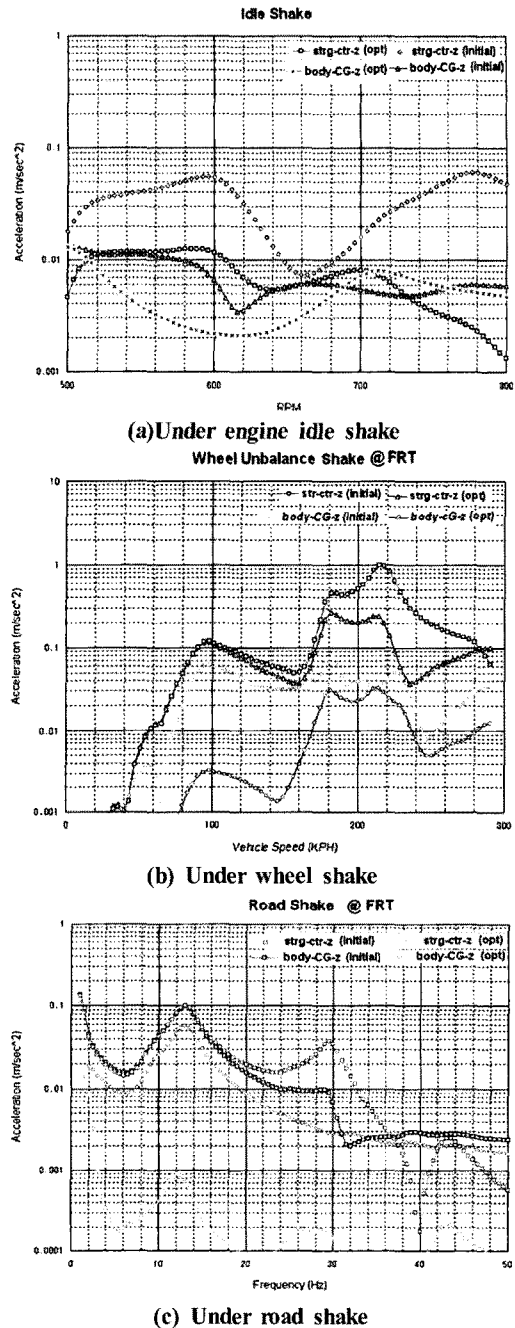


Fig. 12 Acceleration curve of steering wheel and body C.G.

5. Conclusion

This paper presents the integrated process for the model concerning the linear and nonlinear structural stiffness and strength with material strain-hardening. The minimization of strain difference between test and simulation is chosen as the objective function and the corrections of design parameters are based on the various configuration parameters of panel-based structure. The constraints are the dimensional variations of configuration parameters. Body flexibility-based and substructuring simulation with consideration of the coupling specifications can propose very reliable model identification, with the avoidances of over-design of automotive body in the early stage of design. In order to minimize the vibration transferred to the main body structure, the density of kinetic energy due to the vibration must be minimized at several measuring points on the structure. Using the flexibilities among the substructures, the reliable substructure model can be made and the design optimization to such substructure's geometric dimensions and mounting bushing stiffness can effectively be performed.

References

- (1) Huizinga, A. T. M. J. M., Campen, D. H., and Kraker, A., 1997, "Application of Hybrid Frequency Domain Substructuring for Modeling and Automotive Engine Suspension," *Journal of Vibration and Acoustics*, Vol. 119, pp. 304~310.
- (2) Wyckaert, K., Brughmans, M., Zhang, C., and Dupont, R., 1997, "Hybrid Substructuring for Vibro-Acoustical Optimisation: Application to Suspension - Car Body Interaction," *Proceedings of the SAE Noise & Vibration Conference*, pp. 591~598.
- (3) Heo, J. H. and Ehmann, K. F., 1991, "A Method for Substructural Sensitivity Synthesis," *Journal of Vibration and Acoustics*, Vol. 113, pp. 201~208.
- (4) Santos, J. M. C. and Arruda, J. R. F., 1990, "Finite Element Model Updating Using Frequency Response Functions and Component Mode Synthesis," *Proceedings of the International Modal Analysis Conference*, pp. 1195~1201.
- (5) Lallemand, B., Level, P., Duveau, H., and Mahieux, B., 1999, "Eigensolutions Sensitivity analysis using a substructuring method," *Computer & Structures*, Vol. 71, pp. 257~265.
- (6) Jee, T. H., 1995, "*Structural Parameter Identification and Dynamic Modification Using Frequency Response Sensitivity of Substructures*," Ph.D. Thesis, Yonsei University, Korea.
- (7) Ting, T., 1993, "Design Sensitivity Analysis of Structural Frequency Response," *American Institute of Aeronautics and Astronautics Journal*, Vol. 31, pp. 1965~1967.
- (8) Ochsner, S. D. and Bernhard, R. J., 1995, "Application of a component mobility technique to automotive suspension systems," *Noise Control Engineering Journal*, Vol. 43, pp. 73~82.
- (9) Neuwirth, E., Hunter, K., Dittmann, K. J., and Singh, P., 2004, "Experience in use of a virtual test laboratory (VTL) for dynamic multibody simulation (MBS) of full vehicle durability testing," *Numerical Analysis and Simulation in Vehicle Engineering*, Vol. 46, pp. 381~408.
- (10) Stensson, A., Asplund, C., and Karlsson, L., 1994, "The nonlinear behavior of a Macpherson strut wheel suspension," *Vehicle System Dynamics*, Vol. 23, pp. 85~106.
- (11) Yim, H. J. and Lee, S. B., 1996, "An integrated CAE system for dynamic stress and fatigue life prediction of mechanical systems," *KSME Journal*, Vol. 10, No. 2, pp. 158~168.
- (12) Su, H., 2000, "Automotive CAE durability analysis using random vibration approach," *MSC 2nd Worldwide Automotive Conference*, Dearborn, MI, Oct.
- (13) Lee, D. C., Jang, J. H., and Han, C. S., 2006, "Design consideration of mechanical structure with geometric and material non-linearities," *Proc. Instn. Mech. Engrs, Part D; Journal of Automobile Engineering*, Vol. 220, No. 3, pp. 281~288.
- (14) Lee, D. C., 2004, "A design of panel structure for the improvement of dynamic stiffness," *Proc. Instn. Mech. Engrs, Part D; Journal of Automobile*

- Engineering*, Vol. 218, No. 6, pp. 647~654.
- (15) Lee, D. C., Choi, H. S., and Han, C. S., 2006, "Design of automotive body structure using multicriteria optimization," *Struct. Multidisc. Optim.*, Vol. 32, No. 2, pp. 161~167.
- (16) Singiresu, S. Rao, 2002, *Engineering optimization-theory and practice*, 3rd edition, John Wiley & Sons Inc., USA.
- (17) Ding, Y. L., 1986, "Shape optimization of structures: A literature survey," *Computers & Structures*, Vol. 24, No. 6, pp. 985~1004.
- (18) Bendsoe, M. P. and Kikuchi, N., 1988, "Generating optimal topologies for structural design using a homogenization method," *Computer Methods in Applied Mechanics & Engineering*, Vol. 71, pp. 197~224.
- (19) Bendsoe, M. P., 1989, "Optimal shape design as a material distribution problem," *Structural Optimization*, Vol. 1, pp. 193~202.